



ELSEVIER

Nuclear Instruments and Methods in Physics Research B 193 (2002) 516–522

NIM B
Beam Interactions
with Materials & Atoms

www.elsevier.com/locate/nimb

A microcapillary target as a metastable hollow ion source

Y. Yamazaki^{a,b,*}^a Institute of Physics, University of Tokyo, Komaba, Meguro-ku, Tokyo 153-8902, Japan^b Atomic Physics Laboratory, RIKEN, Wako, Saitama 351-0198, Japan

Abstract

Interaction of highly charged ions (HCIs) with solid surfaces has been studied with microcapillary metallic foils, which have many straight holes of ~ 100 nm in diameter and ~ 1 μ m in thickness distributed regularly over the foil. It was found that some considerable fraction of ions can pass through the small capillary without suffering violent collisions with the capillary wall but at the same time capturing multiple electrons in their highly excited Rydberg states, i.e. hollow atoms (ions) are effectively extracted in vacuum. The study of ion–capillary interaction now gets even more promising because of new developments of nano-lithographic techniques, which allow preparing highly ordered microcapillaries. The interaction of HCIs with microcapillaries has been studied through (1) visible light measurements, which provide information on the very beginning of the charge transfer processes, (2) soft X-ray measurements, which reveal the electronic configuration at the moment of inner shell filling processes in a later stage and also (3) angular distribution measurements of each charge-changed component, which provide insight on the position of the ion from the inner wall when the charge transfer takes place. It was found that the ion trajectory is not very much deformed during electron transfers, i.e. one can prepare a well-collimated monoenergetic beam of metastable hollow ions (atoms), which is a unique probe carrying high potential energy at relatively low charge states. © 2002 Elsevier Science B.V. All rights reserved.

PACS: 34.50.Dy

Keywords: Highly charged ions; Microcapillary; Ion–surface interaction; Hollow atom

1. Introduction

The interaction of highly charged ions (HCIs) with a surface has been investigated intensively in the last two decades [1–8], which includes multiple electron transfer processes above and below the surface, high density potential energy deposition

processes, hollow atom formation processes, etc. Intensive studies of both experimental and theoretical aspects have made it possible to construct fundamental scenario of the interaction. It is now widely accepted that the transfer phenomena are well explained with the classical over barrier model [7]. When a HCI approaches a metallic surface, it is further attracted toward the surface due to its image charge. A target electron is resonantly transferred when the distance between the ion and the surface gets less than the critical distance given by $d_c(q) \sim (2q)^{1/2}/W$, where q is the charge and W is the work function of the target, which is of the

* Address: Institute of Physics, University of Tokyo, Komaba, Meguro-ku, Tokyo 153-8902, Japan. Tel.: +81-48-467-9482; fax: +81-48-467-4644.

E-mail address: yasunori@phys.c.u-tokyo.ac.jp (Y. Yamazaki).

order of nm for a typical metal ($W \sim 4\text{--}5$ eV). Such a resonant charge transfer lasts successively till the incident ion is more or less neutralized, i.e. the neutralized ion so produced has many inner shell holes, which is called a hollow atom (ion) of the first generation (HA1) because of this peculiar structure. It is noted that HA1 above the surface is in a nonstationary state forming a molecular orbital with the target, which may more suitably be called a “dynamic hollow molecule” [9]. As can be easily imagined, the HA1 was quite difficult to be produced experimentally until slow HCIs become available, and at the same time has been and still now is quite a challenge to theoretically handle such states. Because the image charge successively accelerates the ion toward the surface until it is neutralized, the HA1 inevitably hits the surface violently. Under a typical experimental condition, the time for the HA1 to exist is very limited ($\sim 10^{-14}\text{--}10^{-13}$ s). If the ion has deep hole(s), the hole(s) can still survive below the surface although quite a short time and then collapse. Such a hollow atom (ion) below the surface is referred to as a hollow atom of the second generation (HA2). Because of this short living time before the collapse, the intrinsic nature of HA1 can only be studied when it is extracted and isolated in vac-

uum. It is noted again that the HA1 is primarily formed via a resonant process, i.e. the HA1 and HA2 keep more or less the initial potential energy of the HCI, which is abruptly released and deposited into a very limited volume of the target during the collapse of HA2.

At least, three principal problems are still left unsolved on the HCI–surface interactions, which are the intrinsic nature of the HA1, the response of atoms/molecules near the target surface during HA1 formation [10,11], and the response of the target during the collapse of HA2 [12]. The present article discusses primarily the first problem, the nature of HA1 employing ion-microcapillary technique, which allows to extract HA1 in vacuum and accordingly allows to study the intrinsic nature of isolated hollow atoms (ions).

2. HCI–microcapillary interaction

To study the HA1 formation process and the intrinsic nature of HA1 avoiding collapse against the solid surface, we have been using a microcapillary foil [13,14], a slice of a bundle of thin straight straws, in which HCIs are shot [9,15,16]. Fig. 1(a) shows three different “fates” of HCIs in the

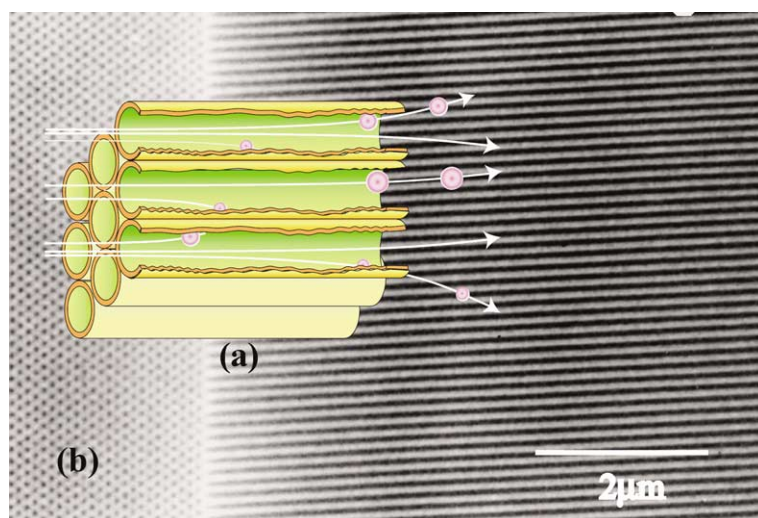


Fig. 1. (a) A schematic drawing of the interaction of HCI and microcapillary and (b) a SEM image of a highly ordered Al_2O_3 microcapillary [14].

capillary depending on their incident positions in the capillary, i.e. (1) when the distance of the HCI to the inner wall is always larger than the critical distance, d_c , the HCI passes through the capillary keeping its initial charge state, (2) when the distance is shorter than d_c , HA1 is formed and then hits the inner wall and collapses, (3) if, however, HA1 is formed near the exit of the capillary, it can escape into the vacuum. Accordingly, the ratio of the charge-changed particles out of all the transmitted particles, f , can be crudely estimated neglecting the influence of the image force as

$$f \sim 2\pi a d_c(q) / \pi a^2 = 2^{3/2} q^{1/2} / aW, \quad (1)$$

where a is the radius of the capillary. Considering that the second charge transfer takes place at $d_c(q-1) \sim (2(q-1))^{1/2}/W$, the charge state distribution at the exit of the capillary, $f_c(q)$, may be given approximately by

$$\begin{aligned} f_c(q) &\sim 2^{3/2} [q^{1/2} - (q-1)^{1/2}] / aW \\ &= 2^{3/2} / [(q^{1/2} + (q-1)^{1/2}) aW]. \end{aligned} \quad (2)$$

The final charge state distribution, $f_f(q)$, which is modified from $f_c(q)$ due to Auger cascading processes, can be obtained by sophisticated theoretical simulations [17,18]. Eq. (2) indicates that the charge state distribution is a monotonically decreasing function of q .

The principal quantum number n_c , in which electron is captured is approximately given by

$$n_c \sim q(2W(1 + (q/8)^{1/2}))^{-1/2}. \quad (3)$$

For HCIs having not very large q (i.e. $(q/8)^{1/2} \sim 1$), $n_c \sim q$ for a metallic target having a typical work function of ~ 4 – 5 eV. Considering that d_c is of the order of nm, Eq. (1) shows that a capillary of 100 nm in diameter can yield a charge transfer fraction of $\sim 1\%$.

Masuda and Fukuda [13] had invented a very sophisticated nano-lithographic technique, which allows fabricating a highly ordered microcapillary foil of Ni and Au. Fig. 1(b) shows a SEM image of an example of the highly order microcapillary made of Al_2O_3 , which has a multitude of straight holes of ~ 50 nm in diameter. It has honeycomb structure with ~ 300 nm interval.

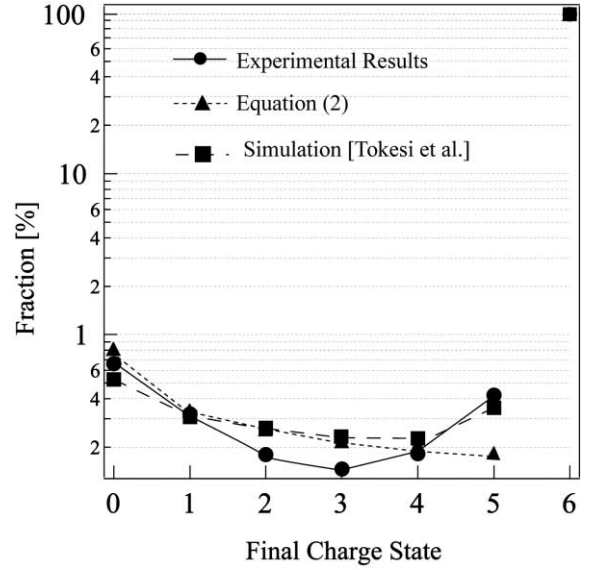


Fig. 2. The charges state distribution of 5 keV/q Xe^{6+} transmitted through a Ni microcapillary [22].

The solid circle in Fig. 2 shows $f_f(q)$ for 5 keV/q Xe^{6+} transmitted through a highly ordered Ni capillary foil. It is noted that the charge state distribution observed here is quite different from that reported for specularly reflected HCIs [19,20] and foil transmitted ions [21]. For example, in the case of glancing scattering of 3.75 keV/u O^{8+} at an Au(110) surface, $\sim 90\%$ of the reflected ions are neutralized, and then the fraction decreases drastically as the exit charge gets larger [19]. It has been found that the U-shape (or “smile”) distribution observed here is universal to all the ions and charge states measured ($3 < q < 13$) [22], which is not in accord with the monotonic decrease expected from Eq. (2) shown by solid triangles in Fig. 2. A key process to bridge this discrepancy is autoionization. The transferred electrons are in highly excited states, and a considerable fraction of them autoionize, which results in reducing the fraction of lower charge state components and increasing the fraction of higher charge state components. As is referred above, Tokesi et al. [17,18] have performed elaborate computer simulations and successfully reproduced the charge state distribution, which is shown by the solid square in Fig. 2.

3. Initial state population

In order to investigate the very beginning of HAI formation process, visible light spectroscopy has been introduced [23,24]. The transition energy $\Delta\varepsilon(\Delta n)$ of an ion with core charge q capturing an electron into a principal quantum number n_c is approximately given by

$$\begin{aligned}\Delta\varepsilon(\Delta n) &\sim -q^2/2n_c^2 + q^2/2(n_c - \Delta n)^2 \\ &\sim q^2\Delta n/n_c^3 \sim \Delta n/q,\end{aligned}\quad (4)$$

where Δn is the difference of the principal quantum number before and after the transition, and $n_c \sim q$ is used. Eq. (4) indicates that visible light is emitted when the incident charge state of the HCI is around 10 for $\Delta n = 1$ transitions. Fig. 3 shows spectra observed when 2 keV/u Ar^{q+} ($q = 6-11$) ions transmitted through a Ni capillary [24]. Most of the strong lines have been successfully attributed to $\Delta n = 1$ transitions of ions captured one electron in the capillary. The numbers in the parentheses, $(n, n-1)$, are the initial and final principal quantum numbers so identified, and the thin solid lines connect a series of transitions having the same initial and final principal quantum numbers for different core charge states. It is seen that strong lines were observed at $n \sim q + 1$ for all the incident charge states studied (for example, $n = 10$ for $q = 9$ and $n = 8$ for $q = 7$).

In order to get quantitative information on the initial state distribution, the spectra were measured with higher resolution so that transitions belonging to different angular momentum quantum number states are distinguished. It was found that major transition lines belong to $l = n - 1$ and $l = n - 2$ states for 2 keV/u Ar^{7+} ions transmitted through a Ni capillary. A cascade analysis revealed that for both $l = n - 1$ and $l = n - 2$ cases, $n = 8$ and $n = 9$ states were very strongly populated [23], i.e. the distribution width of the principal quantum number of the initial states is quite narrow. Eq. (3) predicts that $n_c \sim 8.3$, showing that the average number of the distribution is quite well reproduced with the COB model.

Fig. 3 also shows that transitions with the same wavelengths are observed at two different charge states (e.g. the transitions identified as (10,9) for

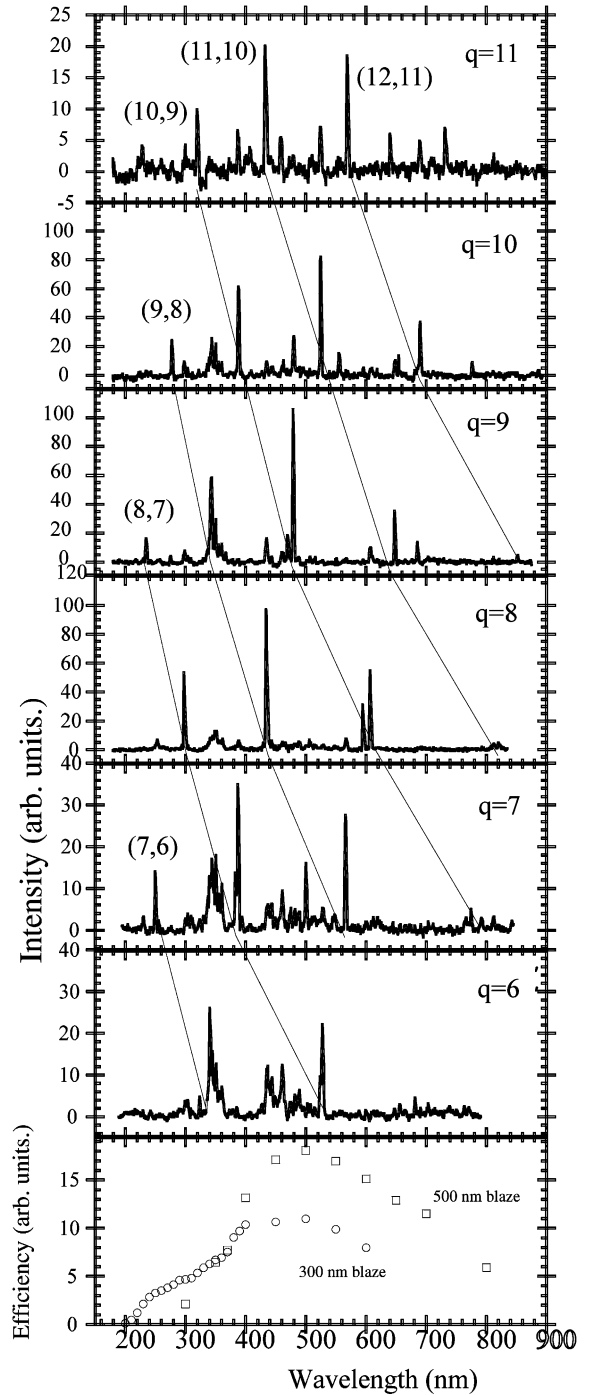


Fig. 3. Visible light spectra for 2 keV/u Ar^{q+} ($q = 6-11$) ions transmitted through a Ni microcapillary [24].

$q = 9$ is also clearly seen for $q = 10$). The broad-band structure around 350 and 450 nm are observed for all the spectra and are attributed to transitions from sputtered Ni atoms, indicating that the inner wall of the capillary is somewhat sputter-cleaned continuously during the experiments.

4. Inner shell vacancy filling process

Soft X-rays emitted from ions transmitted through the capillary have been measured to study the inner shell filling processes [9,15,16]. In contrast to the visible light emission, which probes the early stage of the HA1 evolving freely in vacuum, X-rays probe rather later stage of the HA1. Fig. 4(a) shows the energy spectra of X-rays measured with a Si(Li) detector in coincidence with exiting charge states $q_f = 3, 4$ and 5 for 2.1 keV/u N^{6+} ions transmitted through a Ni capillary [9]. As a reference, an X-ray spectrum observed when HCIs with the same energy hit an flat aluminum plate is shown in the lower part of Fig. 4(a). Although the energy resolution of the Si(Li) detector is not good enough to identify individual core configurations, the peak energies for the capillary transmitted ions are almost the same with each other and are about 30 eV higher than that for the flat Al target, which

indicates that the number of L-shell electrons at the moment of X-ray emission is small and does not depend very much on q_f . Fig. 4(b) shows the decay curve of the X-ray intensities integrated over the energy range shown in Fig. 4(a), which tells that the lifetimes of the N K-shell hole are \sim ns depending only weakly on the exit charge states, which are several orders of magnitudes longer than a typical lifetime of N K-shell vacancy. The observation that the K-shell vacancy is fairly stabilized and the L-shell is not much filled indicates that the spins of K- and L-shell electrons are aligned and accordingly the K-shell filling process is strongly suppressed [9]. Another important observation is the large production ratio of the stabilized states, which are seen from the coincidence yields ($\sim 8\%$, $\sim 4\%$, $\sim 1\%$ and $\sim 0.5\%$ for 2, 3, 4 and 5 electron systems, respectively). In the case of 3 keV/u Ar^{13+} transmitted through a Ni capillary, L-shell lifetimes much longer than 10 ns have been observed [16].

In order to identify the electronic configurations involved in the K-shell filling process with better accuracy, a grating soft X-ray spectrometer combined with a LN_2 cooled CCD was developed [25]. Major core configurations during K X-ray emission were found to be $1s2p^1p$, $1s2p^3p$ and $1s2s2p^4p$ states in the case of 5 keV/u Ne^{9+}

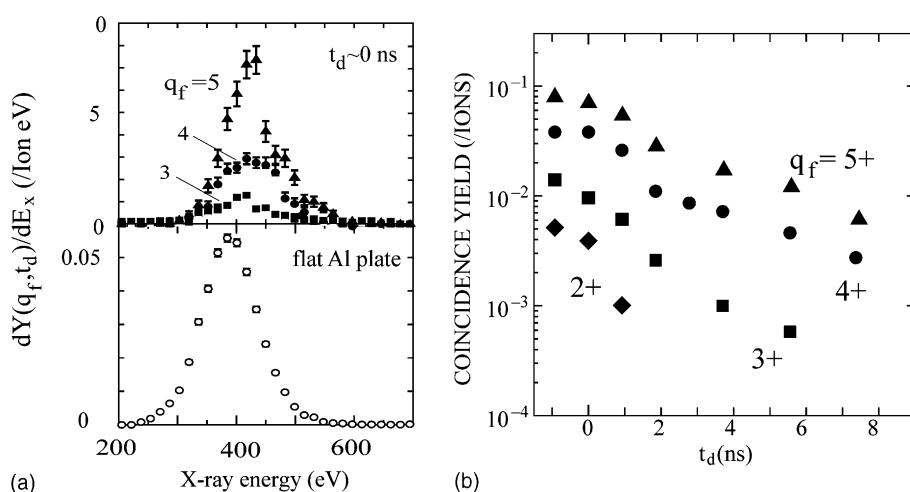


Fig. 4. (a) Energy spectra of N X-rays for 2.1 keV/u N^{6+} ions transmitted through a Ni microcapillary in coincidence with exiting charge state of 5 (▲), 4 (●) and 3 (■). (b) The delayed X-ray yields normalized per one N ion. $q_f = 5$ (▲), 4 (●), 3 (■) and 2 (◆) [9].

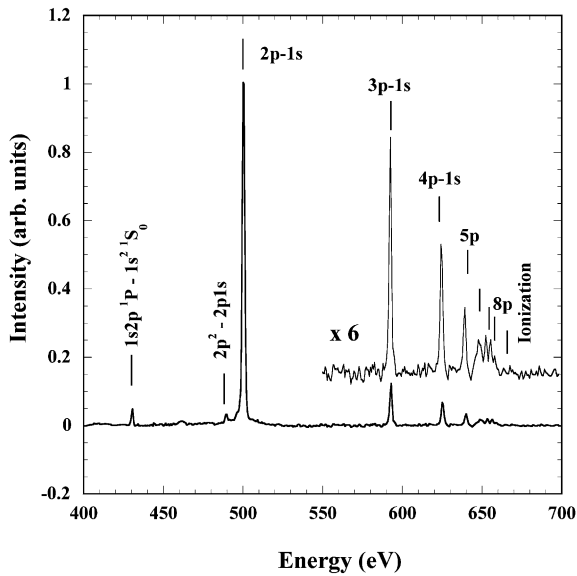


Fig. 5. K X-ray spectrum measured downstream of the target for 2.3 keV/u $^{15}\text{N}^{7+}$ transmitted through a Ni microcapillary foil [26].

transmitted through a Ni capillary [16]. Fig. 5 shows an example of such high resolution X-ray spectra for 2.3 keV/u $^{15}\text{N}^{7+}$ transmitted through a highly ordered Ni capillary [26]. $np-1s$ transitions with n as high as 8 were identified together with $1s2p\ ^1P-1s^2$ and $2p^2-1s2p$ transitions. Considering that the principal quantum number of the initially populated states is $n \sim q + 1$ as discussed in Section 3, the observed $8p-1s$ transition is a transition filling K-shell hole directly from the initially populated state, indicating that even very small angular momentum states are also somewhat populated at least for bare HCIs.

Developments of a superconducting tunnel junction (STJ) X-ray detector are in progress. The energy resolution of the STJ detector is as high as that of the grating spectrometer discussed above and at the same time it delivers timing information, i.e. the STJ detector has the advantage of both the Si(Li) detector and the grating spectrometer combined with the CCD detector [27].

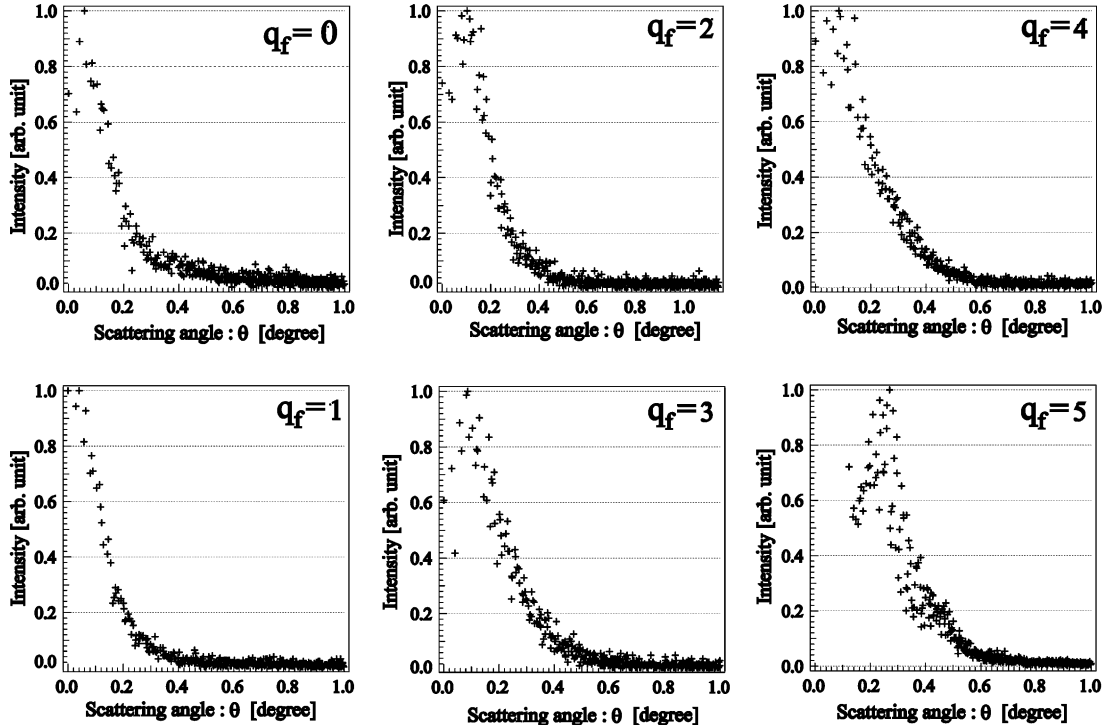


Fig. 6. Scattering angular distribution of 6 keV Xe^{6+} transmitted through a Ni capillary [22].

5. Angular distribution of capillary transmitted HCIs

An angular distribution of HCIs captured electrons in ion–capillary interaction is expected to be broadened and to have a hollow structure due to the image acceleration toward the capillary wall. Fig. 6 shows an example of such an angular distribution for 6 keV Xe⁶⁺ transmitted through a Ni capillary [22]. As is expected, hollow structures are observed for several exiting charge states. However, the hollow structure is more prominent for higher q although theoretical consideration predicts the opposite. Furthermore, the energy gain due to image acceleration, $\Delta\epsilon_{\text{im}}$, is only ~ 200 – 300 meV, which is almost two orders of magnitudes smaller than that expected from the COB model. Experimental [22] and theoretical [17,18,28] studies are in progress to explain this puzzling but interesting observation. An interesting possibility immediately extracted from this observation is to use the stabilized HA1 as a high quality beam keeping high potential energy but with a lower charge state, which may be useful to study a pure potential energy effect particularly on insulator targets.

6. Conclusion

A technique to study the interaction of HCIs with surfaces has been briefly reviewed. The combination of slow HCIs and a microcapillary foil is demonstrated to have a high ability to prepare isolated highly and multiply excited atoms (ions) in stabilized states, which allows to make spectroscopy of various metastable states including multiply charged ions. Further, the fact that the angular distribution of the capillary transmitted ions is very small suggests an interesting possibility to prepare a secondary beam consisting of ions with high potential energy.

Acknowledgements

The author is deeply indebted to H. Masuda, Y. Morishita, Y. Iwai, D. Murakoshi, S. Ninomiya,

K. Tokesi, and J. Burgdoerfer for their collaboration and fruitful discussions.

References

- [1] J.-P. Briand et al., Phys. Rev. Lett. 65 (1990) 159.
- [2] H. Winter, Europhys. Lett. 18 (1992) 207.
- [3] H. Kurz et al., Phys. Rev. Lett. 69 (1992) 1140.
- [4] J. Das, R. Morgenstern, Phys. Rev. A 47 (1993) R755.
- [5] F.W. Meyer et al., Phys. Rev. A 48 (1993) 4479.
- [6] M. Grether et al., Phys. Rev. A 52 (1995) 426.
- [7] J. Burgdoerfer, P. Lerner, F.W. Meyer, Phys. Rev. A 44 (1991) 5674.
- [8] A. Arnau et al., Surf. Sci. Rep. 27 (1997) 113.
- [9] S. Ninomiya, Y. Yamazaki, F. Koiki, H. Masuda, T. Azuma, K. Komaki, K. Kuroki, M. Sekiguchi, Phys. Rev. Lett. 78 (1997) 4557.
- [10] K. Kakutani, T. Azuma, Y. Yamazaki, K. Komaki, K. Kuroki, Jpn. J. Appl. Phys. 34 (1995) L580.
- [11] K. Kuroki, H. Torii, K. Komaki, Y. Yamazaki, Nucl. Instr. and Meth. B 193 (2002) 804.
- [12] T. Schenkel et al., Phys. Rev. Lett. 81 (1998) 2590.
- [13] H. Masuda, K. Fukuda, Science 268 (1995) 1466.
- [14] H. Masuda, H. Yamada, M. Satoh, H. Asoh, M. Nakao, T. Tamamura, Appl. Phys. Lett. 71 (1997) 2770.
- [15] Y. Yamazaki, S. Ninomiya, F. Koike, H. Masuda, T. Azuma, K. Komaki, K. Kuroki, M. Sekiguchi, J. Phys. Soc. Jpn. 65 (1996) 1199.
- [16] Y. Yamazaki, Int. J. Mass Spec. 192 (1999) 437.
- [17] K. Tokesi, L. Wirtz, C. Lemmell, J. Burgdoerfer, Phys. Rev. A 61 (2000) 020901.
- [18] K. Tokesi, L. Wirtz, C. Lemmell, J. Burgdoerfer, Phys. Rev. A 64 (2001) 042902.
- [19] F.W. Meyer, L. Folkert, S. Schippers, Nucl. Instr. and Meth. B 100 (1995) 366.
- [20] N. Hatke et al., Nucl. Instr. Meth. B 115 (1996) 165.
- [21] D. Wikholm, W.S. Bickel, J. Opt. Soc. Am. 66 (1976) 502.
- [22] D. Murakoshi et al., Abstract book of ICPEAC2001, p. 504, and to be published.
- [23] Y. Morishita, S. Ninomiya, Y. Yamazaki, K. Komaki, K. Kuroki, H. Masuda, M. Sekiguchi, Physica Scripta T 80 (1999) 212.
- [24] Y. Morishita et al., Abstract book of egas conference and in press.
- [25] Y. Iwai, S. Thuriiez, Y. Kanai, H. Oyama, K. Ando, R. Hutton, H. Masuda, K. Nishio, K. Komaki, Y. Yamazaki, RIKEN Rev. 31 (2000) 34.
- [26] Y. Iwai et al., Nucl. Instr. and Meth. B 193 (2002) 504.
- [27] H. Ikeda et al., IEEE Trans. Appl. Supercond. 11 (2001) 704.
- [28] K. Tokesi, L. Wirtz, C. Lemmell, J. Burgdoerfer, this conference, in press.